

Circumstellar aluminum oxide and silicon carbide in interplanetary dust particles

Frank J. Stadermann^{a,*}, Christine Floss^a, Brigitte Wopenka^b

^a *Laboratory for Space Sciences and Physics Department, Washington University, St. Louis, MO 63130, USA*

^b *Department of Earth and Planetary Sciences, Washington University, St. Louis, MO 63130, USA*

Received 7 November 2005; accepted in revised form 17 August 2006

Abstract

A systematic NanoSIMS isotope imaging study of sub-micrometer phases in interplanetary dust particles (IDPs) has led to the discovery of two presolar grain types that previously were observed only in primitive meteorites. A $350 \times 600 \text{ nm}^2$ Al_2O_3 grain has a large ^{17}O enrichment and a slight ^{18}O depletion, as well as a ^{26}Mg excess due to the decay of extinct ^{26}Al . Because of its relatively large size and prominent location within the IDP, this presolar Al_2O_3 grain is well characterized by SEM-EDX analyses. A second, much smaller presolar grain has a diameter of 150 nm and a ^{13}C enrichment of more than 300%. Isotopic anomalies in C are rarely found in IDPs and the magnitude of this anomaly is unprecedented. This grain also has a ^{15}N -rich composition and its isotopic makeup as well as its secondary ion yields identify it as a SiC grain. The discovery of presolar Al_2O_3 and SiC in IDPs seamlessly complements earlier notions of interplanetary dust particles as the most primitive extraterrestrial material currently available for laboratory analysis. Both Al_2O_3 and SiC are common presolar grain types in primitive meteorites, but they appeared conspicuously absent from the presolar grain inventory in interplanetary dust particles, which is dominated by silicate stardust. *Not* finding these presolar grain types in interplanetary dust would have been difficult to explain. Abundance estimates of the new presolar grain types in IDPs are hampered by limited statistics, but both Al_2O_3 and SiC are less common than presolar silicates which have been found at relatively high abundances in IDPs. The particle in which these presolar grains have been found belongs to the ‘isotopically primitive subgroup’ of IDPs, yet does not contain any presolar silicates. © 2006 Elsevier Inc. All rights reserved.

1. Introduction

The discovery of preserved presolar grains in meteorites (Anders and Zinner, 1993) has led to the creation of an entirely new field of astrophysical research that connects astronomy with the laboratory study of extraterrestrial materials (Bernatowicz and Zinner, 1997). These presolar grains have isotopic compositions that identify them as stellar condensates that survived prolonged residency in the interstellar medium before being incorporated into Solar System materials some 4.6 billion years ago. The majority and best studied types of presolar grains have been SiC, graphites, and refractory oxides, such as spinel, corundum (Al_2O_3) and hibonite (Zinner, 2004). Recent advances in microanalytical techniques, especially the

development and availability of the NanoSIMS ion microprobe (Hillion et al., 1999; Stadermann et al., 1999; Slodzian et al., 2003), have led to the discovery of presolar silicate grains, initially in IDPs (Messenger et al., 2003a; Floss and Stadermann, 2003) and soon thereafter in primitive meteorites (Mostefaoui and Hoppe, 2004; Nagashima et al., 2004; Nguyen and Zinner, 2004) and in Antarctic micrometeorites (Yada et al., 2005).

Interplanetary dust particles (IDPs) are a unique type of extraterrestrial material available for laboratory analysis. They are samples of the contemporary dust population in the inner solar system and originated from asteroids and short-period (Kuiper belt) comets. IDPs are routinely collected in the stratosphere (Brownlee, 1985) and have been the subject of laboratory studies for more than 20 years. These particles have typical sizes of 5–25 μm and heterogeneous internal compositions on a sub-micrometer scale, which require the use of microanalytical techniques with

* Corresponding author.

E-mail address: fjs@wustl.edu (F.J. Stadermann).

a high spatial resolution. IDPs contain largely unaltered or ‘primitive’ material from the early Solar System and the presolar dust cloud (Bradley et al., 1988; Messenger, 2000) as indicated by their anomalous isotopic compositions. The most commonly observed bulk IDP anomalies are enrichments in D (Zinner et al., 1983; McKeegan et al., 1987; Messenger et al., 1995) and ^{15}N (Stadermann et al., 1989; Messenger et al., 2003b). Many of these isotopic anomalies can be understood as the result of interstellar processes (Zinner, 1988; Sandford et al., 2001). Based on their unique isotopic and mineralogical compositions, it has been argued that IDPs are the most primitive type of extraterrestrial material currently available for laboratory analysis (e.g., Messenger, 2000; Bradley, 2003).

The recent discovery of high abundances of presolar grains in IDPs (Messenger et al., 2003a; Floss et al., 2006) compared to what is found in meteorites further substantiates the primitive nature of this type of extraterrestrial material. It appears that many IDPs and their parent bodies managed to preserve presolar material more efficiently through the life of the Solar System than other material that we have access to. Interestingly, however, most of the presolar grains in IDPs appear to be silicate stardust (Messenger et al., 2003a; Floss et al., 2006) and not the types of presolar grains that are well known from earlier studies of primitive meteorites, such as refractory carbide and oxide grains. *Not* finding any of the ‘classical’ presolar grain types in IDPs would be difficult to explain, as it would require a mechanism to selectively destroy those types of presolar grains while efficiently preserving presolar silicates. The existence of such a destruction mechanism would also be inconsistent with the otherwise extremely low degree of alteration of many IDPs.

Here we report the results of an ongoing NanoSIMS isotope imaging study of IDPs that led to the discovery of circumstellar aluminum oxide (Al_2O_3) and silicon carbide (SiC) subgrains in a previously studied IDP.

2. Experimental

2.1. Sample preparation and initial characterization

The focus of this paper is the IDP U2044-m1-5, nicknamed “Tiberius”, which was originally analyzed as part of a comprehensive ion microprobe study of 65 particles from NASA’s stratospheric collector flags U2 044 and U2 047 (Stadermann et al., 1989, 1990; Stadermann, 1991a,b). For that study, particles were hand-picked from the silicone oil covered collector flags and transferred to a C-coated Nuclepore filter substrate, where the particles were cleansed of the oil for two minutes in a stream of high purity hexane. For an initial characterization, the particles were then analyzed in a JEOL 840A scanning electron microscope (SEM) with an energy dispersive X-ray (EDX) detector. An SEM secondary electron image of IDP Tiberius (Fig. 1) shows a common

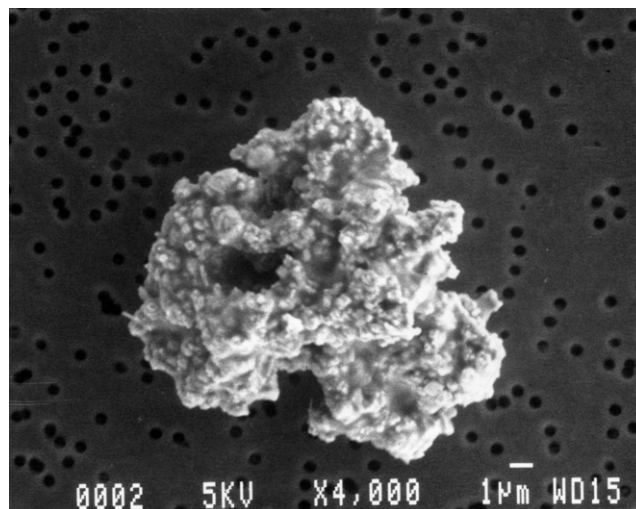


Fig. 1. Electron microscopic picture of IDP Tiberius on a Nuclepore substrate before mounting for SIMS analyses. The original size of this particle was $15 \times 16 \mu\text{m}$.

fine-grained and fluffy (porous) morphology, indicating minimal alteration since its formation. An EDX spectrum of this $15 \mu\text{m}$ -sized non-cluster particle (Fig. 2) indicates a typical chondritic (Schramm et al., 1989) major element composition. Following the SEM characterization, the particles were crushed between quartz disks which typically partitioned the sample material in a ratio of 2:1 on the disks. The larger fraction of each particle was then pressed into high purity Au foil for SIMS analysis. Since the samples get flattened during this step, the available surface areas are typically larger than the particles’ original diameters. In the case of IDP Tiberius, the pressing resulted in two separate fragments on the Au foil. The remaining fraction of IDP Tiberius on the second quartz disk was pressed into a KBr mount for IR transmission measurements. Such measurements frequently allow the identification of the dominant silicate phase in IDPs (Sandford and Walker, 1985), but they were inconclusive in the case of IDP Tiberius.

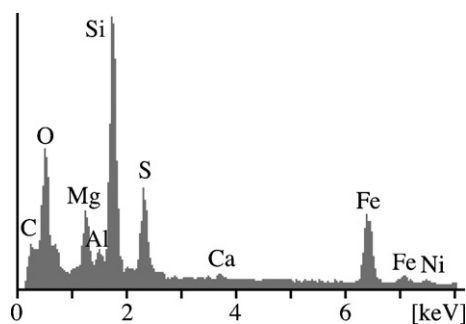


Fig. 2. Bulk SEM-EDX spectrum of IDP Tiberius on the Nuclepore substrate. This major element composition is typical for many IDPs and is commonly referred to as “chondritic”. The spectrum was acquired with a 15 kV primary electron beam.

2.2. Original bulk SIMS studies

Secondary ion mass spectrometry (SIMS) is an analytical technique to determine elemental and isotopic compositions of samples on a size scale that is determined by the diameter of the primary ion beam. Since this beam diameter in most SIMS instruments is on the order of a few micrometers, SIMS is not a ‘bulk’ measurement type in most studies. However, in the analysis of micrometer-sized objects, such as IDPs, the ‘bulk’ size of the sample may be similar to the size of the analysis volume. In such cases, compositional information derived from a SIMS measurement is representative of the sample’s bulk composition. Of the two fragments of IDP Tiberius that were available for SIMS analysis on the Au mount, one was analyzed by the CAMECA ims3f ion microprobe with a 5–10 μm diameter primary beam. This fragment was completely consumed during these SIMS measurements and the ims3f results are representative of the ‘bulk’ composition of this fragment and, likely, of the IDP as a whole.

Hydrogen isotopic ratios (D/H) were measured with a Cs^+ primary ion beam and negative secondary ions. In this mode, isobaric interferences from H_2 are negligible and measurements can be performed at low mass resolution (McKeegan, 1987b). A terrestrial standard of ‘Washington University Amphibole’ with a known isotopic composition (McKeegan, 1987b) was used to correct for effects of instrumental mass fractionation and the results are expressed as delta (δ) values relative to SMOW, standard mean ocean water (Hagemann et al., 1970). In the δ -notation, deviations from the normal isotopic ratio (e.g., $\text{D}/\text{H}_{\text{SMOW}}$) are expressed in parts per thousand (permil, ‰). The isotopic compositions of C and N were determined together in a single measurement with a Cs^+ primary beam and negative secondary ions. Since N does not form stable negative atomic ions, CN^- was measured instead. A moderately high mass resolution of $M/\Delta M = 6000$ was used to separate the mass peaks of $^{12}\text{C}^{15}\text{N}^-$ and $^{11}\text{B}^{16}\text{O}^-$. Measurements of an NBS-21 graphite reference standard were made to calibrate the C isotopic compositions relative to those of Pee-Dee-Belemnite. For N a 1-hydroxy-benzotriazole-hydrate standard was used and the resulting delta values are expressed relative to the N isotopic composition of air. Natural terrestrial samples have been found to exhibit isotopic compositions with $-40\text{‰} < \delta^{13}\text{C} < 0\text{‰}$ (Faure, 1986) and $-8\text{‰} < \delta^{15}\text{N} < 20\text{‰}$ (Geiss and Bochsler, 1982).

In addition to the isotopic measurements, the ims3f ion microprobe was also used for quantitative major and trace element measurements. These measurements were made with an O^- primary beam and positive secondary ions, using low mass resolution and moderate energy filtering (Zinner and Crozaz, 1986). The abundances of 25 elements (Li, Na, Mg, Al, P, S, K, Ca, Sc, Ti, V, Cr, Mn, Fe, Co, Ni, Cu, Zn, Rb, Sr, Y, Zr, Cd, Ba, and Ce) were determined relative to Si, whose absolute abundance was assumed to be CI-chondritic (10.64 wt%). In order to quantify second-

ary ion yields in SIMS measurements, knowledge of mineral-dependent elemental sensitivity factors is generally required. Since IDPs consist of a fine-grained, heterogeneous mix of minerals on a scale that is much smaller than the primary ion beam, averaged sensitivity factors from the measurements of various silicate standards were used for quantification. Despite the limitations resulting from this simplification, the use of averaged sensitivity factors is sufficient for a comparison of IDP Tiberius with other chondritic IDPs, as long as they are measured under the same conditions.

2.3. High spatial resolution NanoSIMS studies

Since there was a significant portion of particle Tiberius left on the Au foil after the original ims3f measurements, it was possible to perform additional analyses with the NanoSIMS on this second fragment of IDP Tiberius, in addition to equivalent measurements on fragments of six other IDPs that were part of the original ims3f study. The NanoSIMS is a new type of SIMS instrument with exceptionally high spatial resolution and sensitivity (Stadermann et al., 1999; Slodzian et al., 2003) which allows isotope ratio imaging at a sub-micrometer scale. This instrument can thus be used to search for isotopically anomalous sub-phases in IDPs that would not have been detectable in the bulk isotopic measurements done with the ims3f SIMS instrument. The analytical approach used in this study is similar to what has previously been described (Floss et al., 2004, 2006; Stadermann et al., 2005). The C, N, O and Si isotopic imaging measurements were made with a 100 nm Cs^+ primary beam of ~ 1 pA with an impact energy of 16 keV. The primary beam was rastered over $10 \times 10 \mu\text{m}^2$ to $20 \times 20 \mu\text{m}^2$ areas of the remaining IDP fragments on the Au substrate. Due to the high C content in the matrix of most IDPs and the fact that the samples are mounted on Au foil, sample charging was no issue in these measurements. Secondary electrons and negative secondary ions were extracted from the sample area, mass separated and detected in parallel, resulting in spatially and temporally correlated secondary electron and ion images in 256^2 or 512^2 pixels. Individual analyses consisted of up to 40 repeated scans across the sample area, with total measurement times up to 7 h. Ion images were then processed following standard procedures (Stadermann et al., 2005). Note that the spatial resolution of the summed-up images is somewhat larger than 100 nm due to minute shifts between the repeated scans and that this results in some mixing with neighboring material in the determination of isotopic ratios. In total, five different detector setups were used for various NanoSIMS measurements of the IDP Tiberius. The detected secondary ion species for the C–O measurements were $^{12}\text{C}^-$, $^{13}\text{C}^-$, $^{16}\text{O}^-$, $^{17}\text{O}^-$ and $^{18}\text{O}^-$ (Setup 1). The mass resolution was set high enough ($m/\Delta m \approx 6500$) to clearly separate isobaric interferences of $^{12}\text{C}^{1}\text{H}^-$ from $^{13}\text{C}^-$ and $^{16}\text{O}^{1}\text{H}^-$ from $^{17}\text{O}^-$. Carbon and O isotope ratio images were then examined for areas

with statistically significant deviations from the normal (solar) ratios of $^{12}\text{C}/^{13}\text{C} = 89$, $^{17}\text{O}/^{16}\text{O} = 3.8 \times 10^{-4}$, and $^{18}\text{O}/^{16}\text{O} = 2.0 \times 10^{-3}$. Bulk particle compositions were used for internal calibration of the isotopic ratios.

Subsequent Mg/Al imaging measurements of IDP Tiberius were made with a 500 nm O^- primary beam and positive secondary ions. Secondary signals of $^{24}\text{Mg}^+$, $^{25}\text{Mg}^+$, $^{26}\text{Mg}^+$, $^{27}\text{Al}^+$, and $^{28}\text{Si}^+$ (Setup 2) were detected in 256^2 pixels in 46 repeated scans over a $10 \times 10 \mu\text{m}^2$ area. Data were then extracted by integrating over visually defined ‘regions of interest’ in the images. An initial $^{26}\text{Al}/^{27}\text{Al}$ ratio was calculated from the observed ^{26}Mg excess following standard procedures (e.g., Nittler et al., 1997) while using the bulk of the particle as internal isotopic standard with an assumed normal Mg isotopic composition.

Measurement of N and Si isotopes in IDP Tiberius was made by scanning a Cs^+ primary beam over a $15 \times 15 \mu\text{m}^2$ area while detecting secondary electrons, $^{12}\text{C}^{14}\text{N}^-$, $^{12}\text{C}^{15}\text{N}^-$, $^{28}\text{Si}^-$, $^{29}\text{Si}^-$ and $^{30}\text{Si}^-$ (Setup 3). Finally, parts of the sample were scanned one more time for anomalies in C, N, and O with parallel secondary ion detection adjusted for $^{12}\text{C}^-$, $^{13}\text{C}^-$, $^{12}\text{C}^{14}\text{N}^-$, $^{12}\text{C}^{15}\text{N}^-$, $^{28}\text{Si}^-$ (Setup 4) and $^{16}\text{O}^-$, $^{17}\text{O}^-$, $^{18}\text{O}^-$, $^{28}\text{Si}^-$, $^{24}\text{Mg}^{16}\text{O}^-$ (Setup 5). All of these measurements were made a sufficiently high mass resolution to resolve the relevant isobaric interferences. For the C and N isotopic measurements, a 1-hydroxy-benzotriazole-hydrate standard, mounted on the same sample holder, was used.

2.4. Raman spectroscopic measurements

During the initial characterization of IDP Tiberius, a fragment of this particle was mounted on KBr for IR measurements (Stadermann, 1991b). The IR spectrum hinted at the presence of layer lattice silicates as the most dominant mineral phase, although the IR spectrum obtained in transmission with an infrared microscope had a low signal to

noise ratio and thus the classification was not conclusive. In an attempt to better constrain the mineralogy (i.e., the crystalline structure) of the material that makes up the bulk of IDP Tiberius, we carried out Raman spectroscopy on the two fragments remaining from the NanoSIMS measurements.

These measurements were performed with a fiber-optically coupled Raman microprobe based on an axial spectrograph with volume holographic transmissions gratings (HoloLab Series 5000 Raman Microscope from Kaiser Optical Systems, Inc.). The excitation light of 532 nm was delivered by a frequency-doubled Nd-YAG laser that is coupled to a Leica microscope via a $8 \mu\text{m}$ single mode optical fiber. An $80\times$ ultra-long working distance objective (NA = 0.75) was used for focusing the light onto the sample with a lateral resolution of $\sim 2 \mu\text{m}$ and a power of 10 mW at the sample surface. The same objective was used for the collection of the scattered light which was focused on the core of a $100 \mu\text{m}$ multi-mode collection fiber. The spectral range of $100\text{--}4000 \Delta\text{cm}^{-1}$ was simultaneously detected with a thermoelectrically cooled CCD array detector with 2048 channels and a spectral resolution of 2.5cm^{-1} . Spectral acquisition time was $64 \times 4 \text{s}$ (times two because of automated γ -ray filtering). The sample was analyzed on the same Au mount used for SIMS analyses and individual micrometer-sized analysis spots were selected and photo-documented while the sample was viewed in reflected visible light on the stage of the Raman microscope.

3. Results

The results of the quantitative bulk trace element measurement of IDP Tiberius are shown in Fig. 3. For comparison, the range of compositions found among a subset of seven IDPs from the original ims3f ion microprobe study is also indicated. This subset of IDPs is comprised of those

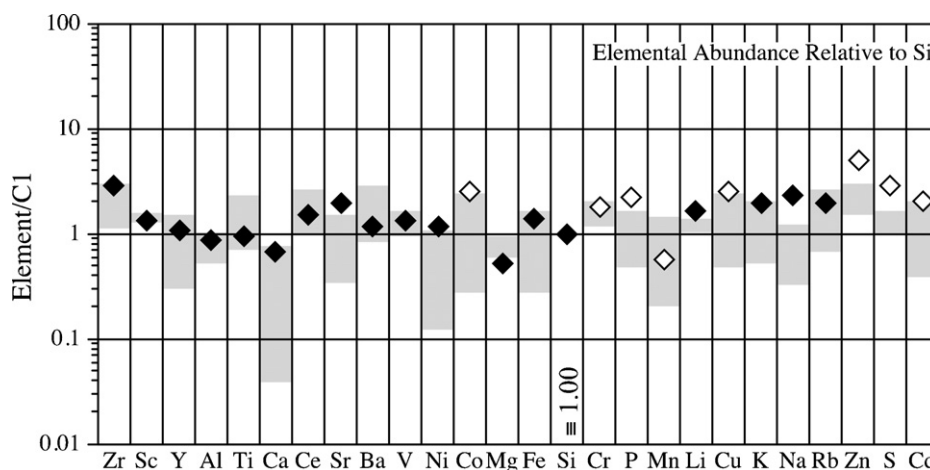


Fig. 3. Bulk major and trace element composition of IDP Tiberius as measured with the ims3f ion microprobe. The abundances are normalized to CI-chondritic abundances and are relative to Si, which was set to “1.00”. Counting statistics 1σ errors are generally smaller than the symbols. Elements are sorted by decreasing condensation temperature (Lodders, 2003) from refractory on the left to more volatile on the right. Open symbols are upper limits, due to the possibility of isobaric molecular interferences on the measured masses. The gray boxes indicate the range of compositions among other previously analyzed chondritic IDPs.

particles whose trace element compositions most closely resemble CI chondritic abundances. The elemental abundances in IDP Tiberius generally fall within the range of compositions seen in the other chondritic IDPs. Some of the apparent deviations from a perfectly chondritic elemental abundance spectrum may be due to the previously discussed problem of using SIMS sensitivity factors for the analysis of IDPs which are heterogeneous on a sub-micrometer scale. In addition, even large IDPs may not contain an average sample of bulk chondritic material. We do not see any evidence for atmospheric entry heating, such as a bulk Zn depletion (Kehm et al., 2002; Flynn et al., 2006), and the IDP Tiberius clearly is not a refractory type particle (Klöck and Stadermann, 1994). Previous trace element studies have found volatile element enrichments in unequilibrated anhydrous IDPs (Flynn et al., 1993, 1994), but it is not clear whether the moderate enrichments of some volatile elements in IDP Tiberius (Fig. 3) are indicative of the same classification.

Two separate measurements of the bulk hydrogen isotopic composition in IDP Tiberius were made with the ims3f ion microprobe. These analyses yielded δD values of $(-15 \pm 50)\text{‰}$ and $(30 \pm 54)\text{‰}$, which are identical within errors and isotopically normal. Bulk C isotopic measure-

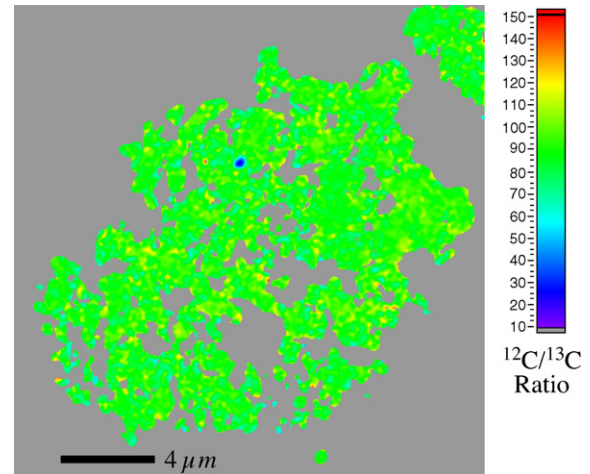


Fig. 7. Results from the C isotopic measurement of a $20 \times 20 \mu\text{m}^2$ area of IDP Tiberius. The false color image shows the range of $^{12}\text{C}/^{13}\text{C}$ ratios in this particle. Areas in solid gray are low in C and therefore did not yield meaningful ratios. The presolar SiC can be recognized by its low $^{12}\text{C}/^{13}\text{C}$ ratio (dark blue). The remainder of the particle has a normal C isotopic composition ($^{12}\text{C}/^{13}\text{C} = 89$) with no statistically significant variations. In this image, the SiC appears larger than it actually is due to image smoothing. A detailed analysis of the NanoSIMS images found the SiC grain to have a diameter of approximately 150 nm.

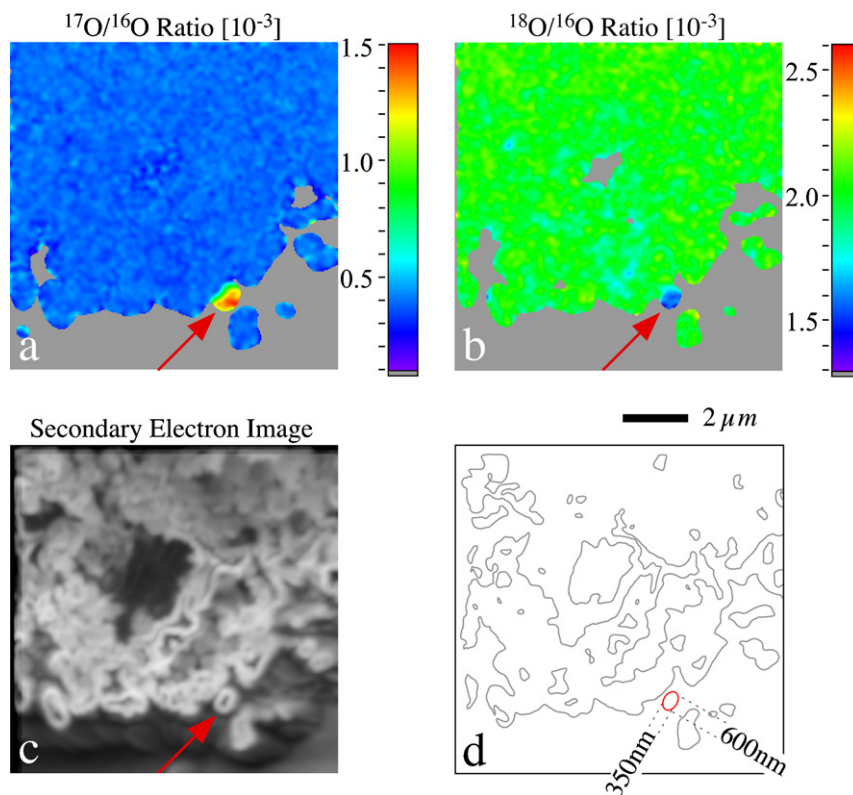


Fig. 4. Results of the NanoSIMS O isotopic measurements of a $10 \times 10 \mu\text{m}^2$ area on a fragment of IDP Tiberius. Images (a) and (b) show false color distributions of O isotopic ratios. Areas in gray are low in O (^{17}O and ^{18}O , respectively) and therefore did not yield meaningful ratios. The presolar Al_2O_3 grain, indicated by the arrows, is clearly distinct in its O isotopic composition from the rest of the analyzed area, which has roughly normal isotopic compositions, *i.e.*, $^{17}\text{O}/^{16}\text{O}_{\text{SMOW}} = 0.38 \times 10^{-3}$ and $^{18}\text{O}/^{16}\text{O}_{\text{SMOW}} = 2.00 \times 10^{-3}$. Image (c) shows the simultaneously acquired secondary electron image of the sample. In the SE contour diagram (d), the size of this grain can be determined as $350 \times 600 \text{ nm}^2$. Note that the diameter of the NanoSIMS primary ion beam and image smoothing leads to a slight augmentation of the apparent grain size in images (a) and (b).

ments in IDP Tiberius showed a slight depletion of ^{13}C relative to PDB with $\delta^{13}\text{C} = (-41 \pm 12)\text{‰}$, which is at the lower end of the range of compositions found in natural terrestrial samples (-40‰ , Faure, 1986). The N isotopic measurement revealed a slight bulk enrichment in ^{15}N with a $\delta^{15}\text{N}$ of $(53 \pm 6)\text{‰}$, well outside of the terrestrial range. No other isotopic measurements were performed on the IDP Tiberius during the original ims3f ion microprobe study. These earlier analyses establish the particle Tiberius as a fairly typical IDP with no unusual characteristics other than the bulk N anomaly. Among the seven IDPs from this study that were later also analyzed with the NanoSIMS, only two (including IDP Tiberius) showed a bulk N anomaly. This is notable because IDPs with bulk N anomalies constitute a group of isotopically primitive IDPs that have a high likelihood of hosting presolar grains (Floss and Stadermann, 2004; Floss et al., 2006).

NanoSIMS imaging measurements of fragments of the same IDPs that were previously studied allow a more detailed look at the particles' internal isotopic makeup. An initial NanoSIMS search for C and O isotopic anomalies was performed on the remaining fragments of IDP Tiberius, as well as of 6 other IDPs that were part of this study. Most of the analyzed areas of IDP Tiberius (and all scanned areas in the additional IDPs) contained no detectable isotopic anomalies in C or O. One area that clearly stood out in the isotope ratio images of O in IDP Tiberius is shown in Fig. 4. The isotopic anomaly is clearly correlated with a well-defined individual grain with a size of $350 \times 600 \text{ nm}^2$. The grain has an isotopic composition of $^{17}\text{O}/^{16}\text{O} = (1.31 \pm 0.03) \times 10^{-3}$ and $^{18}\text{O}/^{16}\text{O} = (1.57 \pm 0.03) \times 10^{-3}$, while the terrestrial ratios are 3.81×10^{-4} and 2.00×10^{-3} , respectively. To evaluate the statistical sig-

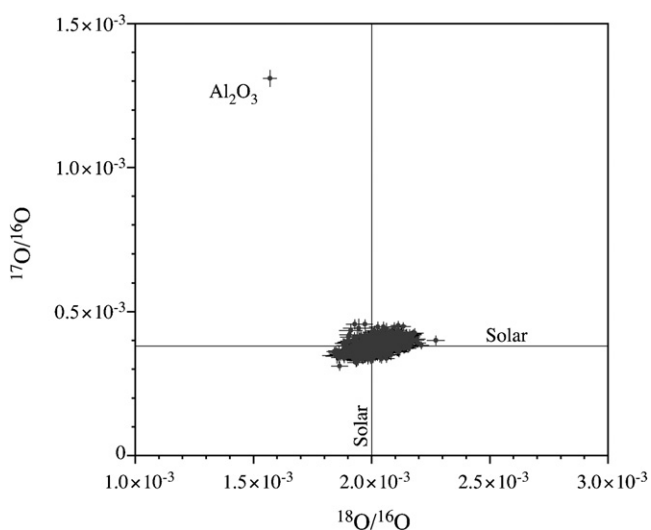


Fig. 5. Three isotope O diagram of the compositions of the Al_2O_3 grain and of 1226 similarly sized regions from other areas of the IDP Tiberius. The error bars shown are 1σ based solely on counting statistics. Areas with low total O signal and correspondingly large errors are excluded. The compositions of the reference areas cluster around the normal (solar) ratios $^{17}\text{O}/^{16}\text{O}_{\text{SMOW}} = 0.38 \times 10^{-3}$ and $^{18}\text{O}/^{16}\text{O}_{\text{SMOW}} = 2.00 \times 10^{-3}$.

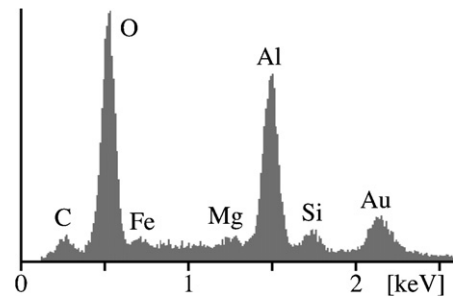


Fig. 6. SEM-EDX spectrum of the presolar Al_2O_3 grain in IDP Tiberius. Although this measurement was made at a relatively low accelerating voltage of 5 kV, there are minor contributions of Au from the substrate as well as of C, Mg, and Fe from neighboring phases. The dominant peaks of O and Al unmistakably identify this grain as Al_2O_3 .

nificance of the observed anomaly, its composition is shown in the $^{17}\text{O}/^{16}\text{O}$ and $^{18}\text{O}/^{16}\text{O}$ three isotope diagram (Fig. 5), where it is compared with other, similar-sized areas in IDP Tiberius, which cluster around the normal O isotopic composition. The O isotopic makeup unmistakably identifies this area as a presolar grain. Such a composition is typical for 'group 1' presolar oxide grains, which are thought to have an origin in red giant and AGB stars (Nittler et al., 1997). The C isotopic composition of this grain ($^{12}\text{C}/^{13}\text{C} = 92 \pm 23$) is normal, although the statistical uncertainty is large due to a very low C abundance.

The prominent location of this grain on the edge of the main sample mass does not give any indication of its original setting within the IDP, since the internal structure was disrupted when the IDP was crushed and pressed into Au. However, the unique location of this isotopic hotspot simplifies its chemical identification, because it reduces the contribution of neighboring phases in the SEM-EDX spectrum. The major element composition in Fig. 6 identifies the anomalous grain as Al_2O_3 , a common presolar grain type in primitive meteorites (e.g., Zinner et al., 2003), although it is not known in this case whether the grain is amorphous Al_2O_3 or crystalline corundum (cf. Stroud et al., 2004). Corundum is only rarely seen in IDPs (McKeegan, 1987a; Zolensky, 1987) and this is the first observation of presolar Al_2O_3 in an IDP. Subsequent Mg/Al isotopic measurements of this grain found an excess in ^{26}Mg due to extinct ^{26}Al , corresponding to an initial $^{26}\text{Al}/^{27}\text{Al}$ ratio of 1.6×10^{-3} . This value is much higher than the $\sim 5 \times 10^{-5}$ upper limit in solar system material (MacPherson et al., 1995), clearly corroborating the presolar origin of this Al_2O_3 grain. Many other 'group 1' presolar oxide grains have similarly high inferred $^{26}\text{Al}/^{27}\text{Al}$ ratios, consistent with their origin from AGB stars after the third dredge-up, which delivers ^{26}Al to the surface (Nittler et al., 1997).

Another isotopically anomalous region shows up in the C isotopic images of IDP Tiberius (Fig. 7). This area has a diameter of 150 nm and a $^{12}\text{C}/^{13}\text{C}$ ratio of 20 ± 2 , corresponding to a $\delta^{13}\text{C}$ of 3450‰ . Due to the small size of the anomalous area in this case and the fact that the sur-

rounding material also contains C, it is likely that the C isotopic composition of the measured area is somewhat diluted with isotopically normal C. Thus, the $^{12}\text{C}/^{13}\text{C}$ ratio and the $\delta^{13}\text{C}$ value can be seen as upper and lower limits, respectively. Isotopic anomalies in C are rarely found in IDPs and the magnitude of this anomaly is unprecedented (Floss et al., 2004, 2006). The C isotopic composition of this grain, which is relatively C-rich, is similar to those of SiC (mainstream or A + B type) from primitive meteorites (Zinner, 2004) and its low O abundance is also consistent with an identification as SiC. The isotopic composition of O from the area of the grain is solar within the large errors ($^{17}\text{O}/^{16}\text{O} = (4.55 \pm 1.29) \times 10^{-4}$ and $^{18}\text{O}/^{16}\text{O} = (2.21 \pm 0.27) \times 10^{-3}$), but the majority—if not all—of the O signal is likely to come from neighboring phases.

To better constrain the type of the SiC grain and its likely origin, the Si and N isotopic compositions were determined in a separate measurement. The area of the grain is Si-rich, but due to the small size of this grain, the analytical errors of the Si isotopic measurement are relatively large. The measured composition of $\delta^{29}\text{Si} = (90 \pm 70)\%$ and $\delta^{30}\text{Si} = (0 \pm 80)\%$ does not show any significant anomalies. The N measurement found a ^{15}N -rich composition in the SiC grain with $^{14}\text{N}/^{15}\text{N} = 91_{-24}^{+52}$, compared to a normal ratio of 272. Since the area surrounding the SiC grain is relatively N-poor, isotopic dilution is not likely to have played as important a role as for the C isotopic measurement. The results of the C and N isotopic measurement are shown in Fig. 8, in comparison with previously established types of presolar SiC grains. If, as discussed above, the actual C isotopic composition of the SiC grain in IDP Tiberius is even more ^{13}C -rich than measured, an identification as A+B type grain becomes most likely. This is also in agreement with the lack of ^{28}Si enrichment that is commonly seen in X-type SiC grains (Zinner, 2004). Since the grain was completely consumed during these measurements, it was not possible to perform further isotopic or elemental characterizations.

In addition to the discovery of these two presolar grains, several other observations were made during the NanoSIMS isotopic characterization of this particle. Through N isotopic imaging, we were able to confirm the ^{15}N -enriched bulk composition of IDP Tiberius that we had expected on the basis of the ims3f measurements. The NanoSIMS data show an average bulk ^{15}N enrichment of $(77 \pm 2)\%$. In addition, like other isotopically primitive IDPs (Floss et al., 2006), particle Tiberius contains several ^{15}N -rich hotspots, as shown in the diagram in Fig. 9. One hotspot (labeled ‘H3’ in Fig. 9) was found during the N and Si imaging measurement and has a $\delta^{15}\text{N}$ of $(1590 \pm 160)\%$, but its C isotopic composition is unknown. The other two hotspots were observed during C and N isotopic imaging. One (‘H1’) has close to normal C with $\delta^{13}\text{C} = (36 \pm 25)\%$, and a moderate ^{15}N enrichment with $\delta^{15}\text{N} = (360 \pm 20)\%$, whereas the other (‘H2’) is strongly enriched in ^{15}N with $\delta^{15}\text{N} = (1900 \pm 210)\%$ and depleted in ^{13}C with $\delta^{13}\text{C} = (-175 \pm 10)\%$. All three ^{15}N hotspots

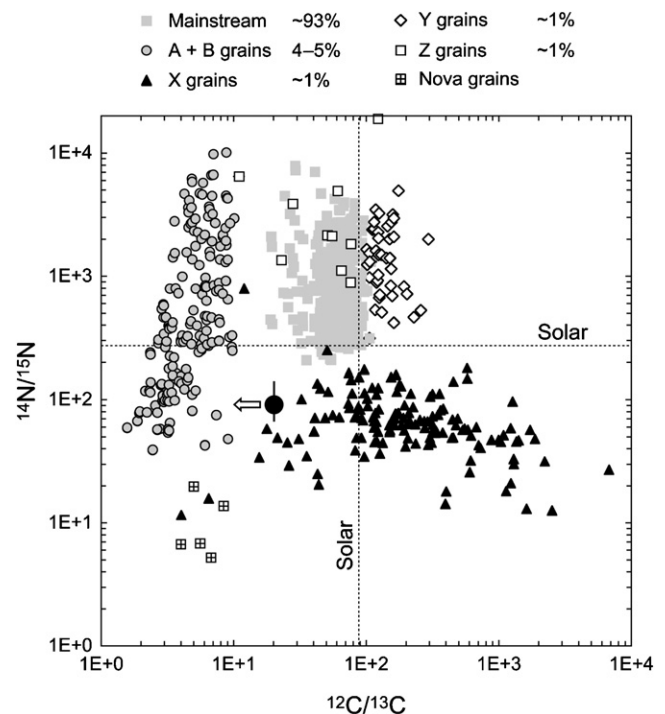


Fig. 8. Carbon and N isotopic composition of the SiC grain in IDP Tiberius (filled black circle) compared to previously established types of presolar SiC. The underlying diagram is from Meyer and Zinner (2006) with grain data from Alexander (1993), Hoppe et al. (1994, 1996, 1997, 2000), Nittler et al. (1995), Huss et al. (1997), Amari et al. (2001a,b,c), and Nittler and Hoppe (2004). The relative percentages of different SiC types is given in the legend, but not shown in their correct proportions in the diagram. Due to the small size of the SiC grain in this study, its measured C isotopic composition is likely diluted with normal C from the surrounding area. Thus, the actual composition of this grain likely is more ^{13}C -rich, as indicated by the arrow.

are relatively large (between 400 and 800 nm in diameter) and are C-rich and depleted in Si. C isotopic anomalies are rare in IDPs and those found to date are all associated with large ^{15}N enrichments (Floss and Stadermann, 2004; Floss et al., 2004, 2006). Most of the ^{15}N enrichments in IDPs are probably not carried by graphite (Floss et al., 2006), but we cannot rule out that a presolar graphite grain is the host phase of the C- and N-anomalous region in IDP Tiberius. Subsequent O isotopic measurements of the areas of the ^{15}N hotspots show normal isotopic compositions.

Although most of the surface area of IDP Tiberius was scanned twice (with detector setups 1 and 5; see Section 2) for variations in its O isotopic compositions, no anomalies—other than of the Al_2O_3 grain—were found. Since O isotopic anomalies are the best indicators for presolar silicates, it appears that this IDP does not contain such grains.

Results from the Raman measurement of IDP Tiberius are shown in Fig. 10, together with reference spectra of olivine, pyroxene, the mica phlogopite and disordered carbonaceous material. Peaks at positions characteristic for minerals with orthosilicate or chain silicate structures were not observed, ruling out the presence of olivine and pyroxene. Rather, the Raman spectrum suggests the presence of

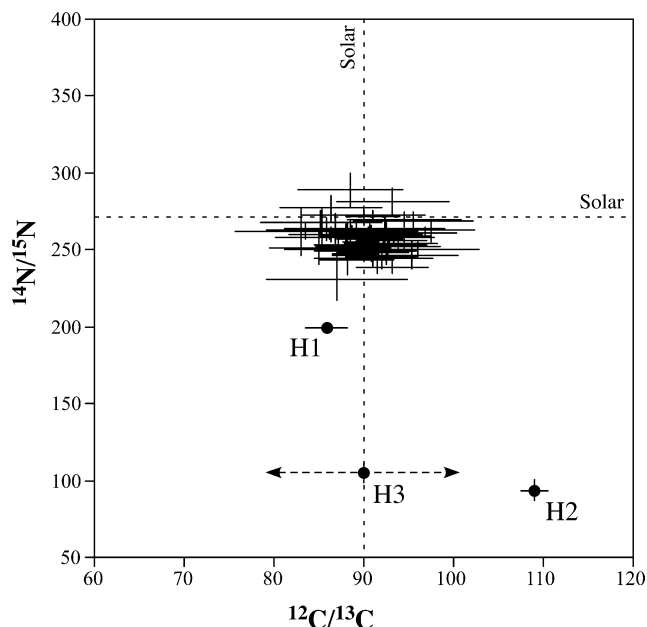


Fig. 9. Carbon and N isotopic compositions of three ^{15}N -rich hotspots (H1, H2, and H3) in IDP Tiberius compared with similarly sized reference areas from elsewhere in the particle. The C isotopic composition of hotspot H3 was not measured; its symbol was arbitrarily placed on the solar value. Note that the bulk composition of IDP Tiberius (as indicated by the reference areas) is slightly enriched in ^{15}N . All error bars shown are 1σ based on counting statistics. Normal compositions are $^{14}\text{N}/^{15}\text{N} = 272$ and $^{12}\text{C}/^{13}\text{C} = 89$.

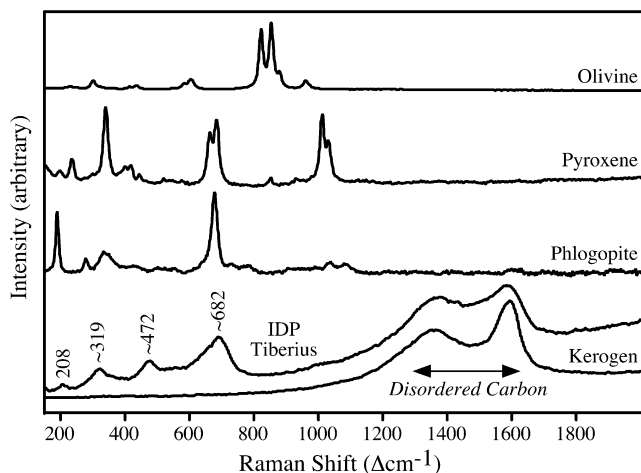


Fig. 10. “Bulk” Raman spectrum of IDP Tiberius compared with spectra of various terrestrial reference minerals. The Si–O peaks below $1000\ \Delta\text{cm}^{-1}$ in the IDP are consistent with a tri-octahedral sheet silicate structure, although no O–H peaks are observed. The wide carbonaceous peaks at ~ 1350 and $\sim 1600\ \Delta\text{cm}^{-1}$ indicate a very disordered structure.

structurally disordered layer lattice silicates, together with highly disordered carbonaceous matter. Most, but not all, terrestrial layer lattice silicates are hydroxyl-bearing, and strong peaks with very characteristic peak positions are typically seen for the O–H stretching vibrations (at $\sim 3500\ \Delta\text{cm}^{-1}$, outside of the spectral range displayed in Fig. 10). However, no peaks for hydroxyl were seen in

the several different micrometer-sized spots analyzed in IDP Tiberius. Despite the fact that the peaks below $1000\ \Delta\text{cm}^{-1}$ are unusually wide (indicating structural disorder or even an amorphous state), their positions are consistent with the Si–O stretching and bending vibrations of sheet silicates with tri-octahedral (rather than di-octahedral) structure. These features suggest that the IDP Tiberius may have originally been dominated by layer lattice silicates that were subsequently heated and dehydrated. The Raman spectra of some heated phyllosilicates do not have any O–H bands, yet are otherwise reminiscent of their original structure, i.e., the characteristic signatures for the di-octahedral and tri-octahedral phyllosilicate structures are preserved after the heating event, even though the peaks become wider (Wopenka et al., 2002). The carbonaceous peaks in Tiberius at ~ 1350 and $\sim 1600\ \Delta\text{cm}^{-1}$ (Fig. 10) are wider and less resolved than even the ones of most terrestrial kerogens (Wopenka and Pasteris, 1993), indicating a very disordered structure.

4. Discussion

The identification of the presolar Al_2O_3 grain in IDP Tiberius is indisputable. This grain has an anomalous O isotopic composition that is rather typical for this type of presolar grain, it is identified as Al_2O_3 by its SEM-EDX spectrum and it also carries evidence for the in situ decay of ^{26}Al , which manifests itself as a ^{26}Mg excess. We do not have any structural information about this grain and are thus hesitant to refer to it as corundum. It has been standard nomenclature in the past to refer to such grains as corundum (Nittler et al., 1997; Zinner, 2004), but recently it has been shown that at least some presolar Al_2O_3 grains have amorphous structures (Stroud et al., 2004).

The arguments for the identification of the second presolar grain in IDP Tiberius as SiC are more circumstantial. The secondary ion yields in the NanoSIMS measurements indicate that the grain is C- and Si-rich, yet poor in O. Its extremely anomalous C isotopic composition is similar to those found in presolar SiC grains in primitive meteorites (e.g., Huss et al., 1997) and it does not contain isotopically anomalous O. In fact, due to its small size of 150 nm, all of the measured O may actually be contributions from the surrounding O-rich material. If, as discussed earlier, the C isotopic composition of the grain is even more ^{13}C -rich than what has been measured (due to isotopic dilution), all isotopic characteristics (heavy N and C, normal Si) point towards an identification as type A + B SiC grain (cf. Fig. 8). This is further validated by abundance arguments, discussed below, since SiC is a relatively abundant type of presolar grain in primitive meteorites. Although some presolar graphites have similar isotopic compositions (e.g., Zinner, 2004), those grains are typically much larger in size ($>1\ \mu\text{m}$) and they do not have the high Si abundance seen in the grain in IDP Tiberius. The reason that SiC has not previously been found in IDPs may be due to the combination of a low abundance and the fact that such grains,

because of their hardness, are easily ‘plucked out’ during the preparation of microtome sections.

Both presolar grains found in IDP Tiberius fit reasonably well into previously established populations of presolar grains from the study of primitive meteorites. The Al_2O_3 grain has a ‘group 1’ O isotopic composition with a large ^{17}O enrichment and a slight ^{18}O depletion, which is indicative of an origin in red giant or asymptotic giant branch stars (Nittler et al., 1997). The observed evidence for the in situ decay of extinct ^{26}Al is also typical for many ‘group 1’ oxide grains, since ^{26}Al from the H burning shell is brought to the surface during third dredge-up episodes in asymptotic giant branch (AGB) stars. A comparison of the O composition in the Al_2O_3 grain with a numerical model (Boothroyd and Sackmann, 1999) is shown in Fig. 11. The composition of the grain from IDP Tiberius is similar to that of the envelope of an AGB star between 1.65 and 1.80 initial solar masses after the first dredge-up, without requiring significant contributions from cool bottom processing (CBP) (Wasserburg et al., 1995). This is consistent with the fact that the observed $^{26}\text{Al}/^{27}\text{Al}$ ratio of 1.6×10^{-3} in the Al_2O_3 grain is only marginally above the value that can be reached in the stellar envelope by normal, CBP-less third dredge-up (Nollett et al., 2003). The measured C isotopic composition of the SiC grain falls between the populations of ‘Mainstream’ and ‘A + B’ SiC

grains. However, if the measured $^{12}\text{C}/^{13}\text{C}$ ratio is indeed diluted with isotopically normal C, as discussed earlier, this SiC grain falls into the group of ^{13}C and ^{15}N -rich ‘A + B’ type SiC grains. These grains make up about 4–5% of the total SiC found in primitive meteorites (Zinner, 2004). Their origin is less well understood than for other types, but J-type carbon stars are the most likely source (Amari et al., 2001c). Even though the isotopic anomalies of the presolar grains in C and O appear massive in these measurements, they contribute only marginally to the bulk C and O isotopic ratios of the particle, due to the small size of the presolar phases.

Abundance estimates of the new presolar grain types in IDPs based on only two grains are statistically meaningless, but both types are less common than presolar silicates which have an abundance of 375 ppm in the isotopically primitive subgroup of IDPs (Floss et al., 2006). By dividing the areas of the presolar phases by the total analyzed area of IDP Tiberius, we infer an abundance of 600 ppm for Al_2O_3 and 60 ppm for SiC in the analyzed fragment of this one IDP. Normalization to the total area of all previously studied IDPs would allow us to calculate the absolute abundances in IDPs, which would be significantly lower. In some primitive meteorites presolar silicates are the most abundant type of circumstellar grains (up to 176 ppm, Nguyen et al., 2005), aside from nanodiamonds. Nanodiamonds have also been found in IDPs, but their origin is still controversial (Dai et al., 2002). Other presolar grain types with abundances in the lower ppm range in primitive meteorites are SiC, oxides, and graphites (Huss, 1997; Zinner, 2004). A discovery of presolar graphite in IDPs is statistically less likely, since its population is dominated by larger ($>1 \mu\text{m}$) grains than other presolar grain types (Croat et al., 2003). Such large grains have a lower detection probability due to the fact that every square- μm of IDP matrix in an isotope imaging measurement can contain hundreds of $\sim 100 \text{ nm}$ (and smaller) grains, but not more than a single $\sim 1 \mu\text{m}$ particle. Based on the high presolar silicate abundance in IDPs, we expect that continued isotope imaging searches will lead to abundance determinations of non-silicate presolar grains in IDPs that are higher than the corresponding values for the matrices of primitive meteorites.

It is surprising that IDP Tiberius contains two presolar grain types that have not previously been seen in IDPs, yet apparently contains no presolar silicates. This may only be a random statistical effect or could be due to preferential loss of presolar silicates in this particle due to aqueous alteration. Both possibilities are discussed below. The IDP Tiberius is a typical representative of the group of chondritic porous IDPs in its morphology, as well as major and trace element abundances. The combination of both the bulk ^{15}N enrichment in IDP Tiberius and the presence of ^{15}N -rich hotspots, unambiguously identify this particle as a member of the isotopically primitive subgroup of IDPs which has the highest concentration of presolar silicates (Floss et al., 2006). To a first approximation, the detection

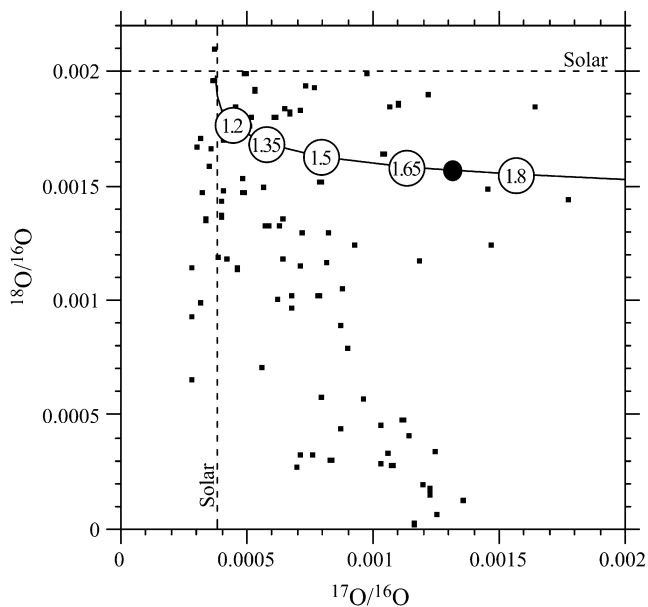


Fig. 11. Oxygen three isotope diagram of presolar grain compositions and model data. The dots indicate compositions of presolar oxide grains from previous studies (Nittler et al., 1997; Choi et al., 1998, 1999; Zinner et al., 2005). The solid line and the numbered circles show model compositions (Boothroyd and Sackmann, 1999) of the envelopes of AGB stars after the first dredge-up for stars of various initial stellar masses (1.2, 1.35, 1.5, 1.65 and 1.8 M_{\odot}) and solar metallicity ($Z = 0.02$). Compositions in the ^{18}O -poor region below the model curve can be reached in the envelope of solar metallicity stars by varying degrees of CBP (Wasserburg et al., 1995). The composition of the Al_2O_3 grain from this study (filled circle) falls directly on the model curve for stars between 1.65 and 1.80 initial solar masses, without requiring CBP.

efficiency for presolar silicates can assumed to be constant as long as the same instrument, matching analytical conditions, identical data reduction techniques and similar sample types are being used. It is thus possible to predict the probability of finding presolar silicates in IDPs by O isotopic imaging with the Washington University NanoSIMS based on the results of previous IDP studies from the same laboratory. Such studies led to the detection of 10 presolar silicates in a total of 3340 μm^2 of searched sample area in the primitive subgroup of IDPs (Floss et al., 2006). The probability to find at least one presolar silicate grain in a scanned area with the size A in a primitive subgroup IDP is then given as

$$100 \cdot \left(1 - e^{-\frac{A}{B}}\right)\%$$

where B is the average area searched for each presolar silicate found in previous studies (i.e., 334 μm^2). Note that this formula is independent of the presolar grain size and that it does not require knowledge of the absolute detection efficiency. The total area of IDP Tiberius that was scanned for O isotopic anomalies in this study was 320 μm^2 , but there is some ambiguity due to the fact that the areas of some individual O isotopic measurements overlapped with one another. Since the C and N isotopic measurements were performed between those overlapping measurements, it is likely that enough material was sputtered away for an essentially new surface area to be exposed. The effective area scanned by O isotopic imaging is estimated to be 400–500 μm^2 , resulting in a probability of ~ 70 –80% to find at least one presolar silicate. Not finding a presolar silicate in the present limited study of IDP Tiberius is statistically conceivable, even if the presolar silicate abundance in this particle is as high as in other primitive subgroup IDPs. However, an alternative explanation for the apparent absence of presolar silicates in IDP Tiberius is discussed below.

The Raman measurements indicate the presence of dehydrated phyllosilicates in this IDP that may be the result of heating at some point during this particle's history. This may have been a parent body event, such as thermal metamorphism or an impact, or it could be due to atmospheric entry heating (Flynn et al., 1994). The latter possibility appears less likely in this case because we do not see any of the telltale signs of atmospheric entry heating, such as a bulk Zn depletion (Kehm et al., 2002). If the phyllosilicates were originally hydrated, then aqueous alteration could account for the apparent absence of presolar silicate grains. Aqueous alteration is more likely to affect presolar silicates than other more refractory presolar phases, either by destroying them or re-equilibrating their oxygen isotopes. This has been observed, for example, in the CR chondrite Renazzo, which contains abundant SiC and matrix material with N isotopic systematics similar to those observed in isotopically primitive IDPs, but does not appear to contain presolar silicates (Floss and Stadermann, 2005).

The similarities with Renazzo may, in addition, indicate a link between the IDP Tiberius and primitive meteorites like the CR chondrites.

The discovery of presolar Al_2O_3 and SiC in IDPs seamlessly complements earlier understanding that presolar grains were part of a widespread reservoir that was incorporated into all solar system bodies and that presolar grain abundances in different materials reflect different degrees of solar system processing (Huss, 1997). Among all currently available types of extraterrestrial materials, the subgroup of isotopically primitive IDPs appears to have undergone the smallest degree of solar system processing, as indicated by their anomalous bulk N compositions and high presolar silicate concentrations (Floss et al., 2006). The new observation that they also contain other common presolar grain types provides additional evidence of their primitive nature.

The extraction of presolar grains from primitive meteorites by acid dissolution (Anders and Zinner, 1993) is still the most efficient way to produce relatively large amounts of certain types of grains, but for in situ studies or the search for new types of presolar materials, IDPs are among the most promising host materials. The return of the first bona fide cometary dust samples by the Stardust mission in 2006 will allow a direct evaluation of the level of preservation of presolar materials in comet 81P/Wild 2. It remains to be seen whether this one comet is chemically and physically representative for the majority of comets or whether the IDP collection, by averaging over a multitude of parent bodies, may actually sample 'more typical' cometary material, assuming a large fraction of IDPs does indeed come from comets.

Acknowledgments

We would like to thank Gary Huss, Larry Nittler, an anonymous reviewer, and Associate Editor Noriko Kita for their careful and helpful reviews. This work was supported by NASA Grant NNG04GG49G to C.F.

Associate editor: Noriko Kita

References

- Alexander, C.M.O'D., 1993. Presolar SiC in chondrites: how variable and how many sources? *Geochim. Cosmochim. Acta* **57**, 2869–2888.
- Amari, S., Gao, X., Nittler, L.R., Zinner, E., José, J., Hernanz, M., Lewis, R.S., 2001a. Presolar grains from novae. *Astrophys. J.* **551**, 1065–1072.
- Amari, S., Nittler, L.R., Zinner, E., Gallino, R., Lugaro, M., Lewis, R.S., 2001b. Presolar SiC grains of type Y: origin from low-metallicity AGB stars. *Astrophys. J.* **546**, 248–266.
- Amari, S., Nittler, L.R., Zinner, E., Lodders, K., Lewis, R.S., 2001c. Presolar SiC grains of type A and B: their isotopic compositions and stellar origins. *Astrophys. J.* **559**, 463–483.
- Anders, E., Zinner, E., 1993. Interstellar grains in primitive meteorites: diamond, silicon carbide, and graphite. *Meteoritics* **28**, 490–514.
- Bernatowicz, T.J., Zinner, E., 1997. Astrophysical Implications of the Laboratory Study of Presolar Materials. In: Bernatowicz, T., Zinner, E. (Eds.), *AIP Conf. Proc.* **402**. AIP, p. 750.

- Boothroyd, A.I., Sackmann, I.-J., 1999. The CNO isotopes: deep circulation in red giants and first and second dredge-up. *Astrophys. J.* **510**, 232–250.
- Bradley, J., 2003. The astromineralogy of interplanetary dust particles. In: Henning, T. (Ed.), *Astromineralogy*. Springer, pp. 217–235.
- Bradley, J.P., Sandford, S.A., Walker, R.M., 1988. Interplanetary dust particles. In: Kerridge, J.F., Matthews, M.S. (Eds.), *Meteorites and the Early Solar System*. University of Arizona Press, pp. 861–895.
- Brownlee, D.E., 1985. Cosmic dust: collection and research. *Annu. Rev. Earth Planet. Sci.* **13**, 147–173.
- Choi, B.-G., Huss, G.R., Wasserburg, G.J., Gallino, R., 1998. Presolar corundum and spinel in ordinary chondrites: origins from AGB stars and a supernova. *Science* **282**, 1284–1289.
- Choi, B.-G., Wasserburg, G.J., Huss, G.R., 1999. Circumstellar hibonite and corundum and nucleosynthesis in asymptotic giant branch stars. *Astrophys. J.* **522**, L133–L136.
- Croat, T.K., Bernatowicz, T., Amari, S., Messenger, S., Stadermann, F.J., 2003. Structural, chemical, and isotopic microanalytical investigations of graphite from supernovae. *Geochim. Cosmochim. Acta* **67**, 4705–4725.
- Dai, Z.R., Bradley, J.P., Joswiak, D.J., Brownlee, D.E., Hill, H.G.M., Genge, M.J., 2002. Possible *in situ* formation of meteoritic nanodiamonds in the early Solar System. *Nature* **418**, 157–159.
- Faure, G., 1986. *Principles of Isotope Geology*. Wiley.
- Floss, C., Stadermann, F.J., 2003. Complementary carbon, nitrogen and oxygen isotopic imaging of interplanetary dust particles: presolar grains and an indication of a carbon isotopic anomaly. *Lunar Planet. Sci.* **XXXIV**, Abstract #1238.
- Floss, C., Stadermann, F.J., 2004. Isotopically primitive interplanetary dust particles of cometary origin: evidence from nitrogen isotopic compositions. *Lunar Planet. Sci.* **XXXV**, Abstract #1281.
- Floss, C., Stadermann, F.J., Bradley, J., Dai, Z.R., Bajt, S., Graham, G., 2004. Carbon and nitrogen isotopic anomalies in an anhydrous interplanetary dust particle. *Science* **303**, 1355–1358.
- Floss, C., Stadermann, F.J., 2005. Presolar (circumstellar and interstellar) phases in Renazzo: the effects of parent body processing. *Lunar Planet. Sci.* **XXXVI**, Abstract #1390.
- Floss, C., Stadermann, F.J., Bradley, J.P., Dai, Z.R., Bajt, S., Graham, G., Lea, A.S., 2006. Identification of isotopically primitive interplanetary dust particles: a NanoSIMS isotopic imaging study. *Geochim. Cosmochim. Acta* **70**, 2371–2399.
- Flynn, G.J., Sutton, S.R., Bajt, S., Klöck, W., Thomas, K.L., Keller, L.P., 1993. The volatile content of anhydrous interplanetary dust. *Meteoritics* **28**, 349.
- Flynn, G.J., Sutton, S.R., Bajt, S., Klöck, W., Thomas, K.L., Keller, L.P., 1994. Hydrated interplanetary dust particles: Element abundances, mineralogies, and possible relationships to anhydrous IDPs. Abstracts of the 25th Lunar and Planetary Science Conf., 381.
- Flynn, G.J., Lanzirotti, A., Sutton, S.R., 2006. Chemical compositions of large cluster IDPs. *Lunar Planet. Sci.* **XXXVII**, Abstract #1216.
- Geiss, J., Bochsler, P., 1982. Nitrogen isotopes in the early solar system. *Geochim. Cosmochim. Acta* **46**, 529–548.
- Hagemann, R., Nief, G., Roth, E., 1970. Absolute isotopic scale for deuterium analysis of natural waters, absolute D/H ratios for SMOW. *Tellus* **22**, 712–715.
- Hillion, F., Horreard, F., Stadermann, F.J., 1999. Recent results and developments on the CAMECA NanoSIMS 50. In: 12th International Conference on Secondary Ion Mass Spectrometry, pp. 209–212.
- Hoppe, P., Amari, S., Zinner, E., Ireland, T., Lewis, R.S., 1994. Carbon, nitrogen, magnesium, silicon and titanium isotopic compositions of single interstellar silicon carbide grains from the Murchison carbonaceous chondrite. *Astrophys. J.* **430**, 870–890.
- Hoppe, P., Strebel, R., Eberhardt, P., Amari, S., Lewis, R.S., 1996. Small SiC grains and a nitride grain of circumstellar origin from the Murchison meteorite: implications for stellar evolution and nucleosynthesis. *Geochim. Cosmochim. Acta* **60**, 883–907.
- Hoppe, P., Annen, P., Strebel, R., Eberhardt, P., Gallino, R., Lugaro, M., Amari, S., Lewis, R.S., 1997. Meteoritic silicon carbide grains with unusual Si-isotopic compositions: evidence for an origin in low-mass metallicity asymptotic giant branch stars. *Astrophys. J.* **487**, L101–L104.
- Hoppe, P., Strebel, R., Eberhardt, P., Amari, S., Lewis, R.S., 2000. Isotopic properties of silicon carbide X grains from the Murchison meteorite in the size range 0.5–1.5 μm . *Meteorit. Planet. Sci.* **35**, 1157–1176.
- Huss, G.R., 1997. The survival of presolar grains in solar system bodies. In: Bernatowicz, T.J., Zinner, E. (Eds.), *Astrophysical Implications of the Laboratory Study of Presolar Materials*. AIP, pp. 721–748.
- Huss, G.R., Hutcheon, I.D., Wasserburg, G.J., 1997. Isotopic systematics of presolar silicon carbide from the Orgueil (CI) carbonaceous chondrite: implications for solar system formation and stellar nucleosynthesis. *Geochim. Cosmochim. Acta* **61**, 5117–5148.
- Kehm, K., Flynn, G.J., Sutton, S.R., Hohenberg, C.M., 2002. Combined noble gas and trace element measurements on individual stratospheric interplanetary dust particles. *Meteorit. Planet. Sci.* **37**, 1323–1335.
- Klöck, W., Stadermann, F.J., 1994. Mineralogical and chemical relationships of interplanetary dust particles, micrometeorites and meteorites. In: Zolensky, M.E., Wilson, T.L., Rietmeijer, F.J.M., Flynn, G.J. (Eds.), *Analysis of Interplanetary Dust*. American Institute of Physics, pp. 51–87.
- Lodders, K., 2003. Solar system abundances and condensation temperatures of the elements. *Astrophys. J.* **591**, 1220–1247.
- MacPherson, G.J., Davis, A.M., Zinner, E.K., 1995. The distribution of aluminum-26 in the early Solar system—a reappraisal. *Meteoritics* **30**, 365–386.
- McKeegan, K.D., 1987a. Oxygen isotopes in refractory stratospheric dust particles: proof of extraterrestrial origin. *Science* **237**, 1468–1471.
- McKeegan, K.D., 1987b. Ion microprobe measurements of H, C, O, Mg, and Si isotopic abundances in individual interplanetary dust particles. Ph.D., Washington University, St. Louis, MO.
- McKeegan, K.D., Swan, P., Walker, R.M., Wopenka, B., Zinner, E., 1987. Hydrogen isotopic variations in interplanetary dust particles. *Lunar Planet. Sci. Conf.* **18**.
- Messenger, S., Clemett, S.J., Keller, L.P., Thomas, K.L., Chillier, X.D.F., Zare, R.N., 1995. Chemical and mineralogical studies of an extremely D-rich IDP. *Meteoritics* **30**, 546–547.
- Messenger, S., 2000. Identification of molecular-cloud material in interplanetary dust particles. *Nature* **404**, 968–971.
- Messenger, S., Keller, L.P., Stadermann, F.J., Walker, R.M., Zinner, E., 2003a. Samples of stars beyond the solar system: silicate grains in interplanetary dust. *Science* **300**, 105–108.
- Messenger, S., Stadermann, F.J., Floss, C., Nittler, L.R., Mukhopadhyay, S., 2003b. Isotopic signatures of presolar materials in interplanetary dust. *Space Sci. Rev.* **106**, 155–172.
- Meyer, B.S., Zinner, E., 2006. Nucleosynthesis. In: Lauretta, D.S., McSween, H.Y., Jr. (Eds.), *Meteorites and the Early Solar System II*. University of Arizona, Tucson, pp. 69–108.
- Mostefaoui, S., Hoppe, P., 2004. Discovery of abundant *in situ* silicate and spinel grains from red giant stars in a primitive meteorite. *Astrophys. J.* **613**, L149–L152.
- Nagashima, K., Krot, A.N., Yurimoto, H., 2004. Stardust silicates from primitive meteorites. *Nature* **428**, 921–924.
- Nguyen, A.N., Zinner, E., 2004. Discovery of ancient silicate stardust in a meteorite. *Science* **303**, 1496–1499.
- Nguyen, A.N., Zinner, E., Stroud, R.M., 2005. Continued characterization of presolar silicate grains from the Acfer 094 carbonaceous chondrite. *Lunar Planet. Sci.* **XXXVI**, Abstract #2196.
- Nittler, L.R., Hoppe, P., Alexander, C.M.O'D., Amari, S., Eberhardt, P., Gao, X., Lewis, R.S., Strebel, R., Walker, R.M., Zinner, E., 1995. Silicon nitride from supernovae. *Astrophys. J.* **453**, L25–L28.
- Nittler, L.R., Alexander, C.M.O'D., Gao, X., Walker, R.M., Zinner, E., 1997. Stellar sapphires: the properties and origins of presolar Al_2O_3 in meteorites. *Astrophys. J.* **483**, 475–495.
- Nittler, L.R., Hoppe, P., 2004. High initial $^{26}\text{Al}/^{27}\text{Al}$ ratios in presolar SiC grains from novae. *Meteorit. Planet. Sci.* **39**, A78.

- Nollett, K.M., Busso, M., Wasserburg, G.J., 2003. Cool bottom processes on the thermally pulsing asymptotic giant branch and the isotopic composition of circumstellar dust grains. *Astrophys. J.* **582**, 1036–1058.
- Sandford, S.A., Walker, R.M., 1985. Laboratory infrared transmission spectra of individual interplanetary dust particles from 2.5 to 25 microns. *Astrophys. J.* **291**, 838–851.
- Sandford, S.A., Bernstein, M.P., Dworkin, J.P., 2001. Assessment of the interstellar processes leading to deuterium enrichment in meteoritic organics. *Meteorit. Planet. Sci.* **36**, 1117–1133.
- Schramm, L.S., Brownlee, D.E., Wheelock, M.M., 1989. Major element composition of stratospheric micrometeorites. *Meteoritics* **24**, 99–112.
- Slodzian, G., Hillion, F., Stadermann, F.J., Horreard, F., 2003. Oxygen isotopic measurements on the CAMECA NanoSIMS 50. *Appl. Surf. Sci.*, 798–801.
- Stadermann, F.J., Walker, R.M., Zinner, E., 1989. Ion microprobe measurements of nitrogen and carbon isotopic variations in individual IDPs. *Meteoritics* **24**, 327.
- Stadermann, F.J., Walker, R.M., Zinner, E., 1990. Stratospheric dust collection: an isotopic survey of terrestrial and cosmic particles. *Lunar Planet. Sci.* **XXI**, 1190–1191.
- Stadermann, F.J., 1991a. Rare earth and trace element abundances in individual IDPs. *Lunar Planet. Sci.* **XXII**, 1311–1312.
- Stadermann, F.J., 1991b. Messung von Isotopen- und Elementhäufigkeiten in einzelnen interplanetaren Staubteilchen mittels Sekundärionen-Massenspektrometrie. Ph.D., University of Heidelberg, Germany.
- Stadermann, F.J., Walker, R.M., Zinner, E., 1999. NanoSIMS: the next generation ion probe for the microanalysis of extraterrestrial material. *Meteorit. Planet. Sci.* **34**, A111–A112.
- Stadermann, F.J., Croat, T.K., Bernatowicz, T.J., Amari, S., Messenger, S., Walker, R.M., Zinner, E., 2005. Supernova graphite in the NanoSIMS: carbon, oxygen and titanium isotopic compositions of a spherule and its TiC sub-components. *Geochim. Cosmochim. Acta* **69**, 177–188.
- Stroud, R.M., Nittler, L.R., Alexander, C.M.O'D., 2004. Polymorphism in presolar Al₂O₃ grains from asymptotic giant branch stars. *Science* **305**, 1455–1457.
- Wasserburg, G.J., Boothroyd, A.I., Sackmann, I.-J., 1995. Deep circulation in red giant stars: a solution to the carbon and oxygen isotope puzzles? *Astrophys. J.* **447**, L37–L40.
- Wopenka, B., Pasteris, J.D., 1993. Structural characterization of kerogens to granulite-facies graphite: applicability of Raman microprobe spectroscopy. *Am. Mineral.* **78**, 533–557.
- Wopenka, B., Popelka, R., Pasteris, J.D., Rotroff, S., 2002. Understanding the mineralogical composition of ancient greek pottery through Raman microprobe spectroscopy. *Appl. Spectrosc.* **56**, 1320–1328.
- Yada, T., Stadermann, F.J., Floss, C., Zinner, E., Olinger, C.T., Graham, G.A., Bradley, J.P., Dai, Z., Nakamura, T., Noguchi, T., Bernas, M., 2005. Discovery of abundant presolar silicates in subgroups of Antarctic micrometeorites. *Lunar Planet. Sci.* **XXXVI**, Abstract #1227.
- Zinner, E., McKeegan, K.D., Walker, R.M., 1983. Laboratory measurements of D/H ratios in interplanetary dust. *Nature* **305**, 119–121.
- Zinner, E., Crozaz, G., 1986. A method for the quantitative measurement of rare earth elements in the ion microprobe. *Int. J. Mass Spectrom. Ion Process.* **69**, 17–38.
- Zinner, E., 1988. Interstellar cloud material in meteorites. In: Kerridge, J.F., Matthews, M.S. (Eds.), *Meteorites and the Early Solar System*. University of Arizona Press, pp. 956–983.
- Zinner, E., Amari, S., Guinness, R., Nguyen, A., Stadermann, F., Walker, R.M., Lewis, R.S., 2003. Presolar spinel grains from the Murray and Murchison carbonaceous chondrites. *Geochim. Cosmochim. Acta* **67**, 5083–5095.
- Zinner, E., 2004. Presolar grains. In: Davis, A.M. (Ed.), *Meteorites, Planets, and Comets*. In: Holland, H.D., Turekian, K.K. (Eds.), *Treatise on Geochemistry*, vol. 1. Elsevier-Pergamon, Oxford, pp. 17–39.
- Zinner, E., Nittler, L.R., Hoppe, P., Gallino, R., Straniero, O., Alexander, C.M.O'D., 2005. Oxygen, magnesium and chromium isotopic ratios of presolar spinel grains. *Geochim. Cosmochim. Acta* **69**, 4149–4165.
- Zolensky, M.E., 1987. Refractory interplanetary dust particles. *Science* **237**, 1466–1468.